THE JOURNAL OF PHYSICAL CHEMISTRY C

Article

Barrier-Less Slow Dissociation of Photogenerated Charge Pairs in High-Performance Polymer-Fullerene Solar Cells

Dimali A. Vithanage, Andrew Barclay Matheson, Vytenis Pranculis, Gordon J Hedley, Scott J. Pearson, Vidmantas Gulbinas, Ifor D. W. Samuel, and Arvydas Ruseckas

J. Phys. Chem. C, **Just Accepted Manuscript** • Publication Date (Web): 01 Jun 2017

ACS Publications

The Journal of Physical Chemistry C is published by the American Chemical Society. 1155 Sixteenth Street N.W., Washington, DC 20036

Barrier-Less Slow Dissociation of Photogenerated Charge Pairs in High-Performance Polymer-Fullerene Solar Cells

*Dimali A. Vithanage[1], Andrew B. Matheson[1], Vytenis Pranculis[2], Gordon J. Hedley[1], Scott J. Pearson[1], Vidmantas Gulbinas[2], Ifor D. W. Samuel[1] , and Arvydas Ruseckas[1]**

[1]*Organic Semiconductor Centre, School of Physics and Astronomy, University of St Andrews, St Andrews, KY16 9SS*

[2] *Center for Physical Sciences and Technology, Saulėtekio av. 3, LT-10257 Vilnius, Lithuania.*

AUTHOR INFORMATION

Corresponding Author

*E-mail: ar30@st-andrews.ac.uk

ABSTRACT. Broadband transient absorption spectroscopy is combined with ultrafast carrier drift measurements to study dissociation of photogenerated charge pairs in efficient photovoltaic blends of the electron donating polymer PTB7 with the acceptor $PC_{71}BM$. The high ensemble-average mobility sum of electrons and holes is observed which is independent of applied electric field above 12 V/μm and indicates nearly barrier-less pair dissociation at room temperature on a picosecond time scale. High efficiency of pair dissociation in this material is achieved by a combination of high electron mobility in fullerene clusters and hole delocalization along the polymer chain which increases by 30% during dissociation. Our results suggest a predominantly diffusive charge pair dissociation mechanism which requires persistent mobility of both carriers and preferably some delocalization of at least one of them.

1. INTRODUCTION

Organic photovoltaic (OPV) solar cells now achieve power conversion efficiencies above 11% and show great potential for low cost manufacturing of large area, lightweight and flexible solar panels.[1-3] The primary photoexcitations in organic materials are tightly bound Frenkel excitons which split into charge pairs by electron or hole transfer across a heterojunction of electron donor and acceptor materials. Because electron transfer is efficient only at short distance of <1 nm and the dielectric constant is generally between 3 and 4, the generated geminate electron-hole pairs are bound by Coulomb attraction. Nevertheless, in optimized structures they dissociate into free charge carriers with nearly 100% efficiency. The mechanism of free carrier generation is still not understood and actively debated.[4-7] Several studies have suggested that ultrafast or even a ballistic charge separation by several nanometers occurs in non-relaxed charge transfer (CT) states in competition with electronic relaxation and vibrational cooling.[8-11] In contrast, recent findings that the internal quantum efficiency of efficient OPV cells is independent of photon energy, including direct excitation

of low energy CT states, suggest that the dissociation of the *relaxed* CT states can be just as efficient as that of the hot CT states.[12-14] The latter arguments are consistent with ultrafast carrier drift measurements in external electric field which can be well described by dissociation of CT states generated on the nearest-neighbour electron donor and acceptor molecules using classical and quantum-mechanical models.[15-17] It has been suggested that there is a gain of Gibbs free energy by separating bound pairs which comes from increased entropy of spatially separated charges and an enthalpy difference of a charge pair in a mixed donor-acceptor phase at the interface and in pure phases of these materials. [6, 8, 18] The important role of entropy is supported by the recent observation that the free carrier yield increases with increasing the time-averaged mobility of slower carriers with only a few exceptions.[19] This implies that electron and hole both have to leave the interface between donor and acceptor to avoid geminate recombination. In order to understand better the role of fast and slow carriers it is important to measure the time-dependent mobility of electrons and holes during pair dissociation.

In this work we use two complementary techniques to study electron and hole motion during charge pair dissociation in an efficient solar cell blend of the conjugated polymer PTB7 with the fullerene derivative $PC_{71}BM$. This blend is a good model material to study charge pair dissociation because it gives devices of 10% efficiency[20-23] and shows very efficient charge pair dissociation and negligible geminate recombination even in the zero electric field.[24, 25-26] We find that electron and hole both move during dissociation of charge pairs but electrons move much faster. We also observe spectral dynamics which suggests that hole delocalization increases when the charge pair dissociates. Our results show the importance of high and persistent carrier mobility up to several nanoseconds in photovoltaic blends and the advantage of conjugated materials which can support charge delocalization.

2. RESULTS

2.1. Transient absorption dynamics. We studied the blend with optimized donor:acceptor ratio 40:60 prepared using 3 vol% of the solvent additive 1,8-diodooctane (DIO) in chlorobenzene solution. Figure 1a shows transient absorption (TA) spectra after excitation at 640 nm. In this case ~70% of the excitation light is absorbed by PTB7 and the remaining 30% by $PC_{71}BM$. A broad photo-induced absorption with a peak at ~1.1 eV appears in less than 1 ps and its peak increases by 30% in 1 ns. We also measured TA spectra after excitation with a shorter wavelength of 515 nm where ~80% of excitation light is absorbed by $PC_{71}BM$ and observed very similar dynamics as shown in Fig. S1 in Supporting Information (SI). This indicates that the slow growth of the TA signal at 1.1 eV does not represent charge generation which we would expect to depend on the excited fractions of the polymer and the fullerene because of the difference in exciton diffusion in two materials and different electron and hole transfer rates. This blend shows an ultrafast decay of fluorescence which suggests that charge generation occurs predominantly in less than 2 ps (see Fig. S2 in SI) and is consistent with previous fluorescence measurements with femtosecond time resolution.[27] These observations and similarity of the TA spectra in Fig. 1a to absorption spectra of chemically doped PTB7 reported in the literature indicate that the measured induced absorption band from 1 ps onwards is dominated by hole polarons.[28-29] A negative TA signal with a peak at ~1.88 eV is caused by ground state bleaching of PTB7 and occurs at slightly higher energy than the peak of ground state absorption in PTB7 at 1.83 eV because of a positive induced absorption band which overlaps with the low energy side of bleaching. The ground state bleaching signal shows no decay over the 1 ns window which indicates that no recombination of photogenerated charges occurs in this time interval at the low excitation energy density (0.5 μJcm^{-2}) used in our experiment. The induced absorption peak shifts with time from 1.13 eV at 1 ps to 1.09 eV at 1 ns which has been observed in previous TA studies.[28-29] No rise of the

TA signal at 1.1 eV was observed in previous studies probably because of the higher excitation densities used, as judged by the 20 times stronger ΔA signals as compared to our measurements.[29] The different dynamics of photo-induced absorption at 1.1 eV and 1.7 eV suggest that they correspond to different electronic transitions in hole polarons. We have fitted the TA kinetics at 1.1 eV to the exponential function $\Delta A = \Delta A_{max}\,[1 - \beta \exp(-kt)]$ with a time-dependent rate constant in a form $k = k_0 t^{-\alpha}$. The best fit gives β=0.3, k(1ps)=11.6 ns^{-1} and α=0.6 which indicates that a 30% rise occurs with a time–dependent rate. This rate is the same with 515 nm and 640 nm excitation (cf. Fig. S1). We also measured transient anisotropy of the PTB7 ground state bleaching following its selective excitation in the blend (Fig. 1c). Initial anisotropy value of 0.4 is observed, which is a theoretical maximum for a two level system consisting of randomly orientated transition dipoles (i.e absorbing chromophores). Anisotropy decays on the 1-1000 ps time scale and indicates hole diffusion from its generation site to a polymer segment with a different orientation. This occurs with a similar rate to that of the rise of the TA signal at 1.1 eV.

2.2. ***Ultrafast carrier drift.*** We have measured the mobility sum of generated electrons and holes using time-resolved electric-field-induced second harmonic generation (TREFISH). In this technique a reverse bias is applied to the solar cell which polarizes the active layer and breaks centro-symmetry for the p-polarized incident light, so that the second harmonic of the probe light (SH) is generated and its intensity shows a quadratic dependence on the electric field F in the active layer. A pump pulse overlaps spatially with the probe and generates electrons and holes which drift in opposite directions in the applied electric field and form electric dipoles which screen the field and hence reduce SH intensity.[30] Several checks have to be carried out for this technique. First, we check that the SH intensity at a flat band condition is negligible. In this case a positive bias is applied to the cell which equals to

the difference of work functions of electrodes, so that the electric field inside the cell is zero. Indeed, we found that in some samples prepared using ITO from different suppliers the SH intensity at a flat band condition was not negligible and we did not use them for drift measurements. The second important check is to make sure that the SH intensity shows a quadratic dependence on the internal electric field. In that case we can be sure that the SH signal originates from the bulk active layer and not from space charges in the active layer or interfaces with electrodes which would cause deviations from the quadratic dependence. We found that the quadratic dependence holds well when a reverse bias is applied in the dark as shown in Fig. S5 in SI. At these conditions all dark charge carriers are extracted from the blend and it works as a dielectric capacitor. All drift measurements are done with a small reverse bias. To avoid a space charge build-up during the measurements it is important that the decrease of the electric field caused by photogenerated charges is much smaller than the applied electric field. For this reason we applied a reverse bias for 10 μsec, synchronized it with a laser pulse and kept the excitation energy density very low at 0.1 μJcm^{-2}. In that case the photo-generated charges reduce the internal electric field by only 5% in 2 ns after excitation and space charge formation is negligible. Every other excitation pulse is blocked by a chopper in order to measure the ratio of SH intensity I_{SH} with excitation pulse and without excitation I_{SH0}. Then the field screening is found using

$$\Delta F/F = (I_{SH}/I_{SH0})^{1/2} - 1 \qquad (1)$$

Figure 2 shows the field screening in the optimized solar cells for different bias. The magnitude of screening increases from about 0.1% at 1 ps to 5% at 2 ns after excitation and is independent of electric bias within a statistical uncertainty of ±5%. This indicates that the mobility of dissociating charge pairs is independent of electric field above 12 V/μm and implies low potential barrier for dissociation of photogenerated charge pairs. This finding is compatible with previous observations that the free carrier yield is independent of electric

field.[24, 25-26] Assuming a uniform electric field across the active layer which will be discussed in the next section, we can relate the field screening in the time interval τ with the integrated discharge photocurrent of the capacitor and hence with the density of generated charge pairs *N(t)* and the sum electron and hole mobilities $\mu(t)$ as

$$\frac{\Delta F(\tau)}{F} = \frac{\Delta Q}{FCL} = \frac{eA}{CL}\int_0^\tau N(t)\mu(t)dt \qquad (2)$$

where $\Delta Q = \int_0^\tau J(t)dt$ is the charge transported by the photocurrent *J(t), C* is the capacitance of the blend, *L* is its thickness between electrodes, *e* is the elementary charge and *A* is the illuminated area of the sample. The *ΔF/F* kinetics measured at *F*=28 V/μm are well described with Equation (2) using the time-dependent carrier mobility $\mu(t) \propto t^{-0.6}$ and only one fitted parameter μ(1ps)=0.12 $cm^2V^{-1}s^{-1}$. Similar and even higher mobility values have been found in other efficient OPV blends and in neat fullerene films at early time after charge generation.[15-16, 31-32] The mobility decreases monotonically to 10^{-3} $cm^2V^{-1}s^{-1}$ at 3 ns which is the time-averaged electron mobility value in $PC_{71}BM$ measured by the time of flight method.[33] This suggests that it takes several nanoseconds for electrons to reach the thermal equilibrium energies at the bottom of inhomogeneous density of states.

3. DISCUSSION

In Section 2.1 we showed that the growth of the TA signal at 1.1 eV and depolarization on the 1-1000 ps time scale represent the dynamics of hole polarons. Based on the particle in a box model the theoretical oscillator strength is expected to scale linearly with the number of π electrons in the molecular box, hence, we attribute a 30% growth of the TA signal at 1.1 eV to a 30% increase in hole delocalization along the polymer chain. The ground state bleaching signal also shows a small growth and a peak shift from 1.89 eV to 1.87 eV with time which is consistent with dynamic hole delocalization. A recent study of hyperfine

interactions of electron spin with protons by electron paramagnetic resonance spectroscopy suggested that holes are delocalized over about 4 nm along the PTB7 chain in spatially separated charge pairs with lifetimes longer than 100 ns at 50 K.[34] Assuming that delocalization of dissociated holes does not change significantly with temperature, an initial hole delocalization over about 3 nm can be estimated at 1 ps after excitation. Hole delocalization helps charge pair dissociation in several ways. For example, Diebel *et al* showed by Monte Carlo simulations that the reduced Coulomb attraction due to the increased initial distance between localized electron and delocalized hole in combination with the high on-chain hole mobility can give efficient pair dissociation at weak electric fields of 10 V/μm but only for hole delocalization over 7 nm or higher.[35] Arkhipov *et al* suggested that electric dipoles formed at the donor-acceptor interface because of partial charge transfer in ground state in combination with oscillating hole in the potential well of the electron can screen the attractive Coulomb potential.[36] These effects are expected to work together with a high carrier mobility which on its own is already sufficient to drive efficient dissociation of charge pairs with just 1 nm initial separation.[16-17]

In Section 2.2 we showed that the field screening and hence the charge carrier mobility are independent of electric field above 12 V/μm. This implies low potential barrier for dissociation of photogenerated charge pairs. This finding is compatible with previous observations that the free carrier yield is independent of electric field.[24, 25-26] Because of field-independent mobility the TREFISH experiment does not distinguish between charge pairs and free carriers.

Next we discuss the role of electron and hole motion in pair dissociation. Anisotropy decay of the ground state bleach occurs with a similar rate to the growth of the TA signal at 1.1 eV and indicates that the increase of hole delocalization occurs simultaneously with hole transport to the polymer chain with a different orientation from the hole generation site (Fig.

1c). The X-ray diffraction studies showed that the orientation correlation length of PTB7 chains in optimized blends with $PC_{71}BM$ is rather short, about 1-1.5 nm,[37] hence the hole depolarization indicates that it diffuses on average only about 1 nm in 1 ns. In Fig. 3 we plot the average hole diffusion length assuming it is proportional to the rise of the 1.1 eV TA signal and depolarization. The total average diffusion distance of both carriers can be estimated using the measured carrier mobility. We found that the mobility sum μ is independent of electric field, so we can use the generalized Einstein relation $D = \mu k_B T/e$ to relate it with carrier diffusivity D, where k_B is the Boltzmann constant, T is temperature and e is the elementary charge[38-39]. Then the mobility value μ=0.12 $cm^2V^{-1}s^{-1}$ at 1 ps determined by TREFISH gives us D=3x10^{-4} cm^2s^{-1}. Because holes move just very short distance in 1 ns, we use a diffusion length in a hemisphere at the two-dimensional donor-acceptor interface to estimate the average diffusion distance of both carriers $r_{diff} = [3\int_0^t D(t)dt]^{1/2}$. The result is plotted in Fig. 3 and shows the carrier diffusion length of about 4 nm in 1 ns. This estimate should be considered as a lower bound because electron delocalization on several fullerene molecules and possible coherent carrier propagation can give a larger carrier diffusion length.[11, 15] We can also estimate an average drift distance of the charge pairs in time t using $r_{drift} = F\int_0^t \mu(t)dt$ which gives us $r_{drift} = 1.5\,nm$ in 1 ns at F=8 V/μm which corresponds to the internal field at short circuit conditions. This is smaller than the estimated diffusion distance by a factor of three showing that diffusion governs charge pair dissociation in solar cells. At the highest field of F=28 V/μm used in the drift measurements the average drift distance is $r_{drift} \approx 5\,nm$ in 1 ns. This distance is very small compared to the thickness of the active layer of 110 nm, hence, our assumption of a uniform electric field across the active layer is valid in Equation 2.

Our estimated carrier diffusion distance of 4 nm in 1 ns is similar to the estimated pair separation distances in other photovoltaic blends on this time scale using a combination of carrier drift measurements and quantum-mechanical modelling,[15] from charge pair recombination dynamics at very low temperature[40] and using electron spin echo.[41] We stress that we have evaluated only an average carrier diffusion distance and do not have information on its distribution function. By subtracting the hole diffusion length, we estimate that electrons diffuse on average 3 nm in 1 ns, hence, electrons are more mobile than holes, especially at early time after pair generation.

In TREFISH experiment we see just a gradual field screening on early time after excitation and no instantaneous charge displacement which would be expected for highly delocalized charges (cf. Fig. S6 in SI). Hole delocalization along the polymer chain is not expected to give a significant displacement because the conjugated PTB7 chains lay predominantly in the plane of the film.[37] If electron was delocalized over many fullerene molecules, we would expect a fast displacement, hence only a small electron delocalization is compatible with our observations. Figure 3 summarises our results with a schematic of hypothetical free energy surfaces. The measured carrier mobility suggests fast electron diffusion which gives an average pair separation of about 2 nm at 1 ps. This pair is loosely bound and stabilized by polarization of the surrounding molecules as well as by hole delocalization along the conjugated polymer chain which further reduces their binding energy, so that they can dissociate by random walk and slow drift on a 10-1000 ps time scale. The external electric field has no effect on the ultrafast carrier drift mobility implying that a potential barrier for pair dissociation is very low. Because it takes several nanoseconds for charge pairs to dissociate into free carriers, it is required that both electrons and holes show a substantial mobility on this time scale to overcome geminate recombination.

4. CONCLUSIONS

We have measured ultrafast carrier drift in optimized PTB7:$PC_{71}BM$ blends following pulsed optical excitation with low energy density. The high ensemble-average mobility sum of electrons and holes is observed which decreases monotonically from 0.12 $cm^2V^{-1}s^{-1}$ at 1 ps to 10^{-3} $cm^2V^{-1}s^{-1}$ at 3 ns. Mobility is independent of applied electric field above 12 V/μm indicating nearly barrier-less pair dissociation at room temperature. A growth of the hole polaron absorption and its depolarization is observed during dissociation which suggest an increase of hole delocalization along the polymer chain and slow hole diffusion. We estimate that electrons diffuse on average about 3 nm in 1 ns, whilst holes diffuse only about 1 nm on the same time scale. Our results show that pair dissociation is a slow process and requires persistent mobility of both carriers and preferably some delocalization of at least one of them. This mechanism is likely to be general in a number polymer-fullerene heterojunctions for photovoltaics.

5. EXPERIMENTAL DETAILS

5.1. Sample preparation. PTB7 with a molecular weight of 92000 Da and a polydispersity of 2.6 was obtained from 1-Material, Inc. $PC_{71}BM$ of 99% purity was obtained from Solenne. PTB7 and fullerene were dissolved in chlorobenzene (HPLC grade from Sigma Aldrich) at a 40:60 ratio by weight and stirred at 50 °C for 4-5 hours. DIO of 3% by volume (Sigma-Aldrich) was added to the solution which was then stirred for other 5 min. Blended films for transient absorption spectroscopy were prepared by spin-coating on clean fused silica substrates at 1000 r.p.m. in the nitrogen-filled glove box. Solar cells for carrier drift measurements were prepared on an indium-tin oxide coated glass substrate. First a ~60 nm layer of PEDOT:PSS was deposited by spin-coating. Then a PTB7:fullerene blend layer of

110 nm was spin-coated on it at 1000 r.p.m. The layers of calcium (~20 nm) and aluminium (~100 nm) were subsequently deposited by vacuum sublimation. The structure was encapsulated with a glass coverslip and epoxy. The power conversion efficiency (PCE) of the fresh prepared devices was 5.4% at AM1.5 conditions and about 5% after the optical measurements were completed.

5.2. Transient absorption measurements. The schematic of the pump-probe set-up is shown in Supporting Information. The pump was by 180 fs light pulses from an optical parametric amplifier pumped by Pharos laser (from Light Conversion) at 2.5 kHz. Optically delayed pulses of white light continuum generated in YAG crystal are used for the probe. The probe light was optically filtered to attenuate the fundamental 1030 nm wavelength, dispersed by a prism after the sample and detected with a photodiode array. The sample was kept in vacuum during measurements and the pump energy density was 0.5 μJcm^{-2}.

5.3. Carrier drift measurements. The schematic of the TREFISH set-up is shown in Supporting Information. A p-polarized probe light pulsed at 1 kHz and 800 nm is shone on a cell at ~45° incidence angle. A reverse bias is applied through a load resistor of 10 kOhm for about 100 microseconds. Pump pulses at 680 nm wavelength are generated by an optical parametric amplifier and chopped at 500 Hz. They overlap spatially with the probe and generate charge pairs which drift in response to electric field and so they screen the field. The field screening is found by taking a ratio of SH intensities with and without pump pulse. The time delay between pump and probe pulse is varied by an optical delay line. The pump energy density was 0.1 μJcm^{-2}.

ASSOCIATED CONTENT

Supporting Information. Absorption spectra of PTB7 and $PC_{71}BM$, Transient absorption kinetics with different excitation wavelengths, Time-resolved fluorescence data, Transient absorption set-up, Set-up for ultrafast carrier drift measurements, EFISH signal dependence on the total electric field and time. This material is available free of charge on the ACS publications website.

ACKNOWLEDGMENTS

The work in St Andrews was supported by the Engineering and Physical Sciences Research Council (grants EP/L017008/1, EP/J009016/1 and EP/G03673X/1) and the European Research Council (grant 321305). The work in Vilnius was supported by the Research Council of Lithuania (project MIP-85/2015). I.D.W.S. acknowledges support from a Royal Society Wolfson Research Merit Award. D.A.V. is grateful to Supergen SuperSolar Hub for the travel grant. The research data supporting this publication can be accessed at http://dx.doi.org/10.17630/7ec84b4b-d2ab-493c-aaf6-5503a44c0eb5

References

(1) Lu L.; Zheng T.; Q., W.; M., S. A.; Zhao D.; Yu, L.. Recent Advances in Bulk Heterojunction Polymer Solar Cells. *Chem. Rev.* **2015,** *115*, 12666-12731.

(2) Li, S.; Ye, L.; Zhao, W.; Zhang, S.; Mukherjee, S.; Ade, H.; Hou, J. Energy-Level Modulation of Small-Molecule Electron Acceptors to Achieve over 12% Efficiency in Polymer Solar Cells. *Adv. Mat.* **2016,** *28*, 9423-9429.

(3) Baran, D.; Ashraf, R. S.; Hanifi, D. A.; Abdelsamie, M.; Gasparini, N.; Röhr, J. A.; Holliday, S.; Wadsworth, A.; Lockett, S.; Neophytou, M.; et al. Reducing the efficiency–stability–cost gap of organic photovoltaics with highly efficient and stable small molecule acceptor ternary solar cells. *Nat. Mat.* **2017,** *16*, 363–369.

(4) Bassler, H.; Kohler, A. "Hot or cold": how do charge transfer states at the donor-acceptor interface of an organic solar cell dissociate? *Phys. Chem. Chem. Phys.* **2015,** *17*, 28451-28462.

(5) Few, S.; Frost, J. M.; Nelson, J. Models of charge pair generation in organic solar cells. *Phys. Chem. Chem. Phys.* **2015,** *17*, 2311-2325.

(6) Gao, F.; Inganas, O. Charge generation in polymer–fullerene bulk-heterojunction solar cells. *Phys. Chem. Chem. Phys.* **2014,** *16*, 20291-20304.

(7) Hedley, G. J.; Ruseckas, A.; Samuel, I. D. W. Light Harvesting for Organic Photovoltaics. *Chem. Rev.* **2017,** *117*, 796-837.

(8) Clarke, T. M.; Ballantyne, A.; Shoaee, S.; Soon, Y. W.; Duffy, W.; Heeney, M.; McCulloch, I.; Nelson, J.; Durrant, J. R. Analysis of Charge Photogeneration as a Key Determinant of Photocurrent Density in Polymer: Fullerene Solar Cells. *Adv. Mat.* **2010,** *22*, 5287–5291.

(9) Bakulin, A. A.; Rao, A.; Pavelyev, V. G.; Loosdrecht, P. H. M. v.; Pshenichnikov, M. S.; Niedzialek, D.; Cornil, J.; Beljonne, D.; Friend, R. H. The Role of Driving Energy and Delocalized States for Charge Separation in Organic Semiconductors. *Science* **2012,** *335*, 1340-1344.
(10) Gélinas, S.; Rao, A.; Kumar, A.; Smith, S. L.; Chin, A. W.; Clark, J.; Poll, T. S. v. d.; Bazan, G. C.; Friend, R. H.; . Ultrafast Long-Range Charge Separation in Organic Semiconductor Photovoltaic Diodes. *Science* **2014,** *343*, 512-516.
(11) Savoie, B. M.; Rao, A.; Bakulin, A. A.; Gelinas, S.; Movaghar, B.; Friend, R. H.; Marks, T. J.; Ratner, M. A. Unequal Partnership: Asymmetric Roles of Polymeric Donor and Fullerene Acceptor in Generating Free Charge. *J. Am. Chem. Soc.* **2014,** *136*, 2876-2884.
(12) Lee, J.; Vandewal, K.; Yost, S. R.; Bahlke, M. E.; Goris, L.; Baldo, M. A.; Manca, J. V.; Van Voorhis, T. J. Charge transfer state versus hot exciton dissociation in polymer-fullerene blended solar cells. *J. Am. Chem. Soc.* **2010,** *132*, 11878-11880.
(13) Vandewal, K.; Albrecht, S.; Hoke, E. T.; Graham, K. R.; Widmer, J.; Douglas, J. D.; Schubert, M.; Mateker, W. R.; Bloking, J. T.; Burkhard, G. F.; et al. Efficient charge generation by relaxed charge-transfer states at organic interfaces *Nat. Mat.* **2014,** *13*, 63-68.
(14) Hofstad, T. G. J. v. d.; Nuzzo, D. D.; Berg, M. v. d.; Janssen, R. A. J.; Meskers, S. C. J. Influence of Photon Excess Energy on Charge Carrier Dynamics in a Polymer-Fullerene Solar Cell. *Adv. Energy Mater.* **2012,** *2*, 1095-1099.
(15) Abramavicius, V.; Pranculis, V.; Melianas, A.; Inganäs, O.; Gulbinas, V.; Abramavicius, D. Role of coherence and delocalization in photo-induced electron transfer at organic interfaces. *Sci. Rep.* **2016,** *6*, 32914.
(16) Vithanage, D. A.; Devizis, A.; Abramavičius, V.; Infahsaeng, Y.; Abramavičius, D.; MacKenzie, R. C. I.; Keivanidis, P. E.; A.Yartsev; Hertel, D.; Nelson, J.; Sundström, V.; Gulbinas, V. Visualizing charge separation in bulk heterojunction organic solar cells. *Nat. Commun.* **2013,** *4*, 2334.
(17) Abramavicius, V.; Vithanage, D. A.; Devizis, A.; Infahsaeng, Y.; Bruno, A.; Foster, S.; Keivanidis, P. E.; Abramavicius, D.; Nelson, J.; Yartsev, A.; Sundstrom, V.; Gulbinas, V. Carrier motion in as-spun and annealed P3HT:PCBM blends revealed by ultrafast optical electric field probing and Monte Carlo simulations. *Phys. Chem. Chem. Phys.* **2014,** *16*, 2686-2692.
(18) Gregg, B. A. Entropy of charge separation in organic photovoltaic cells: The benefit of higher dimensionality. *J. Phys. Chem. Lett.* **2011,** *2*, 3013-3015.
(19) Stolterfoht, M.; Armin, A.; Shoaee, S.; Kassal, I.; Burn, P.; Meredith, P. Slower carriers limit charge generation in organic semiconductor light-harvesting systems. *Nat. Commun.* **2016,** *7*, 11944.
(20) Liang, Y.; Xu, Z.; Xia, J.; Tsai, S.; Wu, Y.; Li, G.; Ray, C.; Yu, L. For the Bright Future—Bulk Heterojunction Polymer Solar Cells with Power Conversion Efficiency of 7.4%. *Adv. Mat.* **2010,** *22*, E135–E138.
(21) He, Z.; Zhong, C.; Su, S.; Xu, M.; Wu, H.; Cao, Y. Enhanced power-conversion efficiency in polymer solar cells using an inverted device structure. *Nat. Photon.* **2012,** *6*, 591-595.
(22) Liu, Y.; Zhao, J.; Li, Z.; Mu, C.; Ma, W.; Hu, H.; Jiang, K.; Lin, H.; Ade, H.; Yan, H. Aggregation and morphology control enables multiple cases of high-efficiency polymer solar cells *Nat. Commun.* **2014,** *5*, 5293.
(23) Ouyang, X.; Peng, R.; Ai, L.; Zhang, X.; Ge, Z. Efficient polymer solar cells employing a non-conjugated small-molecule electrolyte. *Nat. Photon.* **2015,** *9*, 520–524.
(24) Pranculis, V.; Ruseckas, A.; Vithanage, D. A.; Hedley, G. J.; Samuel, I. D. W.; Gulbinas, V. Influence of Blend Ratio and Processing Additive on Free Carrier Yield and Mobility in PTB7:PC71BM Photovoltaic Solar Cells. *J. Phys. Chem. C* **2016,** *120*, 9588-9594.
(25) Foertig, A.; Kniepert, J.; Gluecker, M.; Brenner, T.; Dyakonov, V.; Neher, D.; Deibel, C. Nongeminate and Geminate Recombination in PTB7:PCBM Solar Cells. *Adv. Mat.* **2013,** *24*, 1306–1311.
(26) Kniepert, J.; Lange, I.; Heidbrink, J.; Kurpiers, J.; Brenner, T. J. K.; Koster, L. J. A.; Neher, D. Effect of Solvent Additive on Generation, Recombination, and Extraction in PTB7:PCBM Solar Cells: A Conclusive Experimental and Numerical Simulation Study. *J. Phys. Chem. C* **2015,** *119*, 8310-8320.

(27) Hedley, G. J.; Ward, A. J.; Alekseev, A.; Howells, C. T.; Martins, E. R.; Serrano, L. A.; Cooke, G.; Ruseckas, A.; Samuel, I. D. W. Determining the optimum morphology in high-performance polymer-fullerene organic photovoltaic cells *Nat. Commun.* **2013,** *4*, 2867.

(28) Rolczynski, B. S.; Szarko, J. M.; Son, H. J.; Liang, Y.; Yu, L.; Chen, L. X. Ultrafast Intramolecular Exciton Splitting Dynamics in Isolated Low-Band-Gap Polymers and Their Implications in Photovoltaic Materials Design. *J. Phys. Chem. C* **2012,** *134*, 4142-4152.

(29) Yonezawa, K.; Kamioka, H.; Yasuda, T.; Han, L.; Moritomo, Y. Exciton-to-Carrier Conversion Processes in a Low-Band-Gap Organic Photovoltaic. *Jpn. J. Appl. Phys.* **2013,** *52*, 062405.

(30) Devizis, A.; Serbenta, A.; Meerholz, K.; Herte, D.; Gulbinas, V. Ultrafast dynamics of carrier mobility in a conjugated polymer probed at molecular and microscopic length scales. *Phys. Rev. Lett.* **2009,** *103*, 027404.

(31) Pranculis, V.; Inhafaseng, Y.; Tang, Z.; Devižis, A.; Vithanage, D. A.; Ponseca, C. S.; Inganäs, O.; Yartsev, A. P.; Gulbinas, V.; Sundström, V. Charge carrier generation and transport in different stoichiometry APFO3:PC61BM solar cells *J. Am. Chem. Soc.* **2014,** *136*, 11331-11338.

(32) Devižis, A.; Hertel, D.; Meerholz, K.; Gulbinas, V.; Moser, E. Time-independent, high electron mobility in thin PC61BM films: relevance to organic photovoltaics. *Org. Electron.* **2014,** *15*, 3729-3734.

(33) Ebenhoch, B.; Thomson, S. A. J.; Genevičius, K.; Juška, G.; Samuel, I. D. W. Charge carrier mobility of the organic photovoltaic materials PTB7 and PC71BM and its influence on device performance. *Org. Electron.* **2015,** *22*, 62-68.

(34) Niklas, J.; Mardis, K. L.; Banks, B. P.; Grooms, G. M.; Sperlich, A.; Dyakonov, V.; Beaupré, S.; Leclerc, M.; Xu, T.; Yu, L.; Poluektov, O. G. Highly-efficient charge separation and polaron delocalization in polymer–fullerene bulk-heterojunctions: a comparative multi-frequency EPR and DFT study. *Phys. Chem. Chem. Phys.* **2013,** *15*, 9562-9574.

(35) Deibel, C.; Strobel, T.; Dyakonov, V. Origin of the Efficient Polaron-Pair Dissociation in Polymer-Fullerene Blends. *Phys. Rev. Lett.* **2009,** *103*, 036402.

(36) Arkhipov, V. I.; Heremans, P.; Bassler, H. Why is Exciton Dissociation So Efficient at the Interface Between a Conjugated Polymer and an Electron Acceptor? *Appl. Phys. Lett.* **2003,** *82*, 4605−4605.

(37) Hammond, M. R.; Kline, R. J.; Herzing, A. A.; Richter, L. J.; Germack, D. S.; Ro, H.; Soles, C. L.; Fischer, D. A.; Xu, T.; Yu, L.; Toney, M. F.; DeLongchamp, D. M. Molecular Order in High-Efficiency Polymer/Fullerene Bulk Heterojunction Solar Cells. *ACS Nano* **2011,** *5*, 8248-8257.

(38) Wetzelaer, G. A. H.; Koster, L. J. A.; Blom, P. W. M. Validity of the Einstein Relation in Disordered Organic Semiconductors. *Phys. Rev. Lett.* **2011,** *107*, 066605.

(39) Nenashev, A. V.; Jansson, F.; Baranovskii, S. D.; Osterbacka, R.; Dvurechenskii, A. V.; Gebhard, F. Effect of Electric Field on Diffusion in Disordered Materials II. Two- and Three-dimensional Hopping Transport. *Phys. Rev. B* **2009,** *81*, 115204.

(40) Barker, A. J.; Chen, K.; Hodgkiss, J. M. Distance Distributions of Photogenerated Charge Pairs in Organic Photovoltaic Cells. *J. Am. Chem. Soc.* **2014,** *136*, 12018-12026.

(41) Lukina, E. A.; Popov, A. A.; Uvarov, M. N.; Kulik, L. V. Out-of-Phase Electron Spin Echo Studies of Light-Induced Charge-Transfer States in P3HT/PCBM Composite. *J. Phys. Chem. B* **2015,** *119*, 13543-13548.

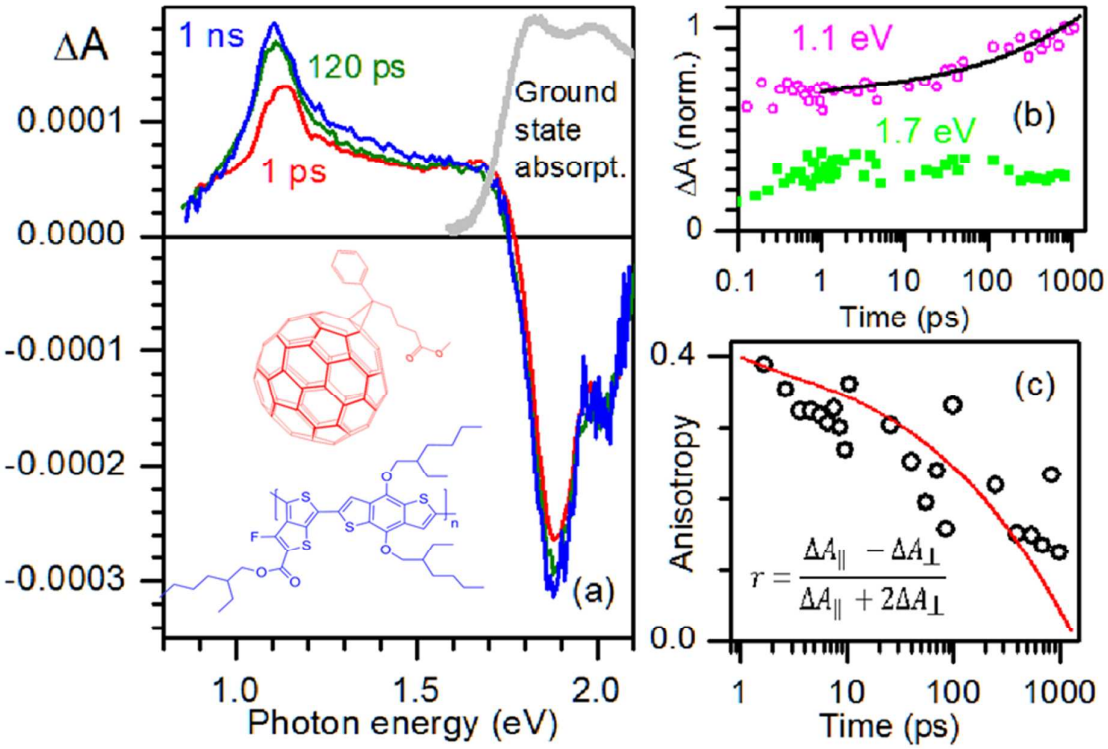

Figure 1. TA results of an optimized blend of 40 wt% PTB7 and 60 wt% $PC_{71}BM$ prepared with DIO; (a) TA spectra at different time delays (1 ps, 120 ps and 1 ns) after excitation at 640 nm with pulse energy density of 0.5 μJcm^{-2}. The grey line shows the ground state absorption spectrum. Chemical structures of $PC_{71}BM$ and PTB7 are shown in the inset. (b) TA kinetics at selected probe photon energies. Solid line shows a fit of the 1.1 eV kinetics to a function $\Delta A = \Delta A_{max}\,[1 - \beta \exp(-kt)]$ where $k = k_0 t^{-\alpha}$ which gives β=0.3, k(1ps)=11.6 ns^{-1} and α=0.6. (c) Transient anisotropy of the ground state bleaching signal at 1.8 eV after excitation at 1.6 eV calculated from TA signals measured with parallel ($\Delta A_{\parallel}$) and perpendicular ($\Delta A_{\perp}$) polarizations of the pump and probe light using the equation shown in the inset. Solid line shows a scaled function $r \propto \exp(-kt)$ with the same parameters as in (b).

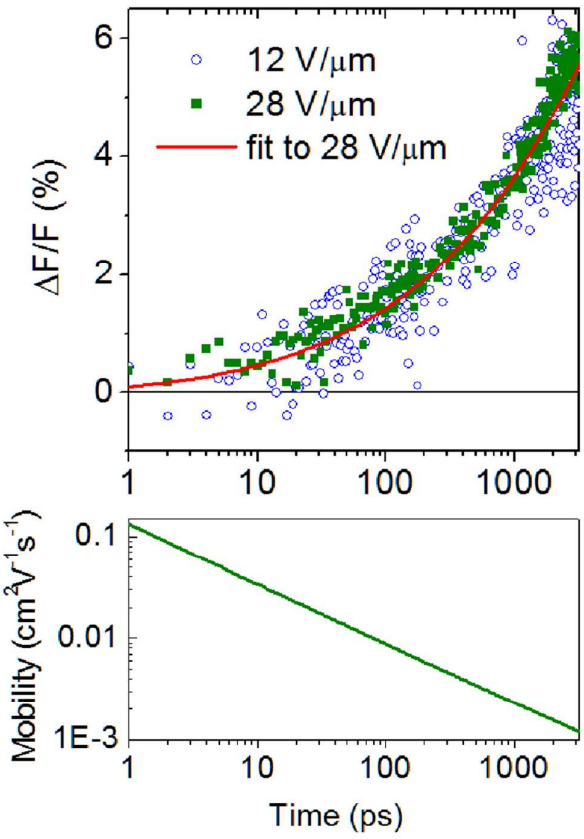

Figure 2. Time-resolved screening of the applied electric field by drift of photogenerated charge pairs in the optimized blend of 40 wt% PTB7 with $PC_{71}BM$ for different field values. The field strength is determined by $F=(V_{appl}+V_{bi})/L$ where V_{appl} is the applied external voltage and V_{bi} is the built-in potential which we take equal to the difference of the work functions of the electrodes (V_{bi} = 0.88 V) and L is the thickness of the blend between electrodes (in this case L=110 nm). Solid line is a fit using Equation (2) with a time-dependent mobility shown in the bottom panel. Excitation pulse energy density was 0.1 μJcm^{-2} at 680 nm.

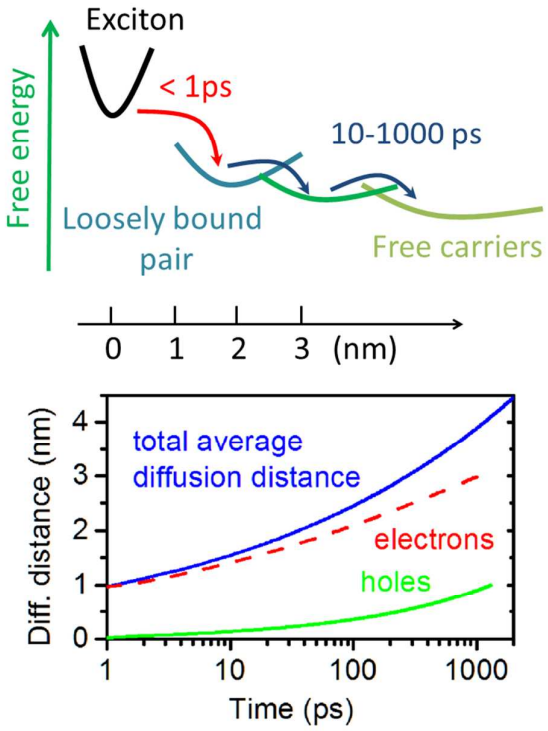

Figure 3. A schematic of the charge separation mechanism in optimized PTB7 blends with $PC_{71}BM$ as suggested by our results. Loosely bound pair of delocalized hole and electron is generated within 1 ps and dissociates by carrier diffusion without experiencing Coulomb binding barrier. The bottom panel shows the estimated mean diffusion distances of electrons and holes and their sum as described in the text.

TOC GRAPHIC